Atmospheric
Chemistry
and Physics

On the diurnal, weekly, and seasonal cycles and annual trends in atmospheric CO_2 at Mount Zugspitze, Germany, during 1981–2016

Ye Yuan[1], **Ludwig Ries**[2], **Hannes Petermeier**[3], **Thomas Trickl**[4], **Michael Leuchner**[1,5], **Cédric Couret**[2], **Ralf Sohmer**[2], **Frank Meinhardt**[6], **and Annette Menzel**[1,7]

[1]Department of Ecology and Ecosystem Management, Technical University of Munich (TUM), Freising, Germany
[2]German Environment Agency (UBA), Zugspitze, Germany
[3]Department of Mathematics, Technical University of Munich (TUM), Garching, Germany
[4]Institute of Meteorology and Climate Research, Atmospheric Environmental Research (IMK-IFU),
Karlsruhe Institute of Technology (KIT), Garmisch-Partenkirchen, Germany
[5]Springer Nature B.V., Dordrecht, the Netherlands
[6]German Environment Agency (UBA), Schauinsland, Germany
[7]Institute for Advanced Study, Technical University of Munich (TUM), Garching, Germany

Correspondence: Ye Yuan (yuan@wzw.tum.de)

Abstract. A continuous, 36-year measurement composite of atmospheric carbon dioxide (CO_2) at three measurement locations on Mount Zugspitze, Germany, was studied. For a comprehensive site characterization of Mount Zugspitze, analyses of CO_2 weekly periodicity and diurnal cycle were performed to provide evidence for local sources and sinks, showing clear weekday to weekend differences, with dominantly higher CO_2 levels during the daytime on weekdays. A case study of atmospheric trace gases (CO and NO) and the passenger numbers to the summit indicate that CO_2 sources close by did not result from tourist activities but instead obviously from anthropogenic pollution in the near vicinity. Such analysis of local effects is an indispensable requirement for selecting representative data at orographic complex measurement sites. The CO_2 trend and seasonality were then analyzed by background data selection and decomposition of the long-term time series into trend and seasonal components. The mean CO_2 annual growth rate over the 36-year period at Zugspitze is 1.8 ± 0.4 ppm yr^{-1}, which is in good agreement with Mauna Loa station and global means. The peak-to-trough amplitude of the mean CO_2 seasonal cycle is 12.4 ± 0.6 ppm at Mount Zugspitze (after data selection: 10.5 ± 0.5 ppm), which is much lower than at nearby measurement sites at Mount Wank (15.9 ± 1.5 ppm) and

Schauinsland (15.9 ± 1.0 ppm), but following a similar seasonal pattern.

1   Introduction

Long-term records of atmospheric carbon dioxide (CO_2) improve our understanding of the global carbon cycle, as well as long- and short-term changes, especially at remote background locations. The longest continuous measurements of atmospheric CO_2 started in 1958 at Mauna Loa, Hawaii, initiated by investigators of the Scripps Institution of Oceanography (Pales and Keeling, 1965). The measurements were performed on the north slope of the Mauna Loa volcano at an elevation of 3397 m above sea level (a.s.l.), thus at long distances from CO_2 sources and sinks. Later, additional measurement sites were established for background studies of global atmospheric CO_2, such as the South Pole (Keeling et al., 1976), Cape Grim, Australia (Beardsmore and Pearman, 1987), Mace Head, Ireland (Bousquet et al., 1996), and Baring Head, New Zealand (Stephens et al., 2013). Along with sites located in Antarctica or along coastal/island regions, continental mountain stations offer excellent options to observe background atmospheric levels due to high elevations that are less affected by local influences, for example,

Mount Waliguan, China (Zhang et al., 2013), Mount Cimone, Italy (Ciattaglia, 1983), Jungfraujoch, Switzerland, and Puy de Dôme, France (Sturm et al., 2005).

Although mountainous sites experience less impact from local pollution and represent an improved approach to background conditions compared with stations at lower elevations, we cannot fully dismiss the influence of local to regional emissions. This influence largely depends on airmass transport and mixing within the moving boundary layer height. Lidar measurements show that air from the boundary layer is orographically lifted to approximately 1–1.5 km above typical summit heights during daytime in the warm season (Carnuth and Trickl, 2000; Carnuth et al., 2002). A 14-year record of atmospheric CO_2 at Mount Waliguan (3816 m a.s.l.), China, reveals significant diurnal cycles and depleted CO_2 levels during summer that are mainly driven by biological and local influences from adjacent regions, although the magnitude and contribution of these influences are smaller than those at other continental or urban sites (Zhang et al., 2013). At the Mt. Bachelor Observatory (2763 m a.s.l.), USA, atmospheric CO_2 variations were studied in the free troposphere and boundary layer separately, where wildfire emissions were observed to drive CO_2 enhancement at times (McClure et al., 2016). However, it still remains unclear to exactly what extent elevated mountain sites are influenced by local activities and how to characterize better local sources and sinks at such stations. It is difficult to make quantitative conclusions on the anthropogenic and biogenic contributions to these measurements (Le Quéré et al., 2009). Analyzing weekly periodicity may be a potential indicator since periodicity represents anthropogenic activity patterns during 1 week (7 days) without the influence of natural causes (Cerveny and Coakley, 2002). From the perspective of modeling and satellite observational systems, studies have shown that the weekly variability has implications on the quantification and verification of anthropogenic CO_2 emissions, as well as diurnal variability (e.g., Nassar et al., 2013; Liu et al., 2017). Regarding in situ measurements, results from Ueyama and Ando (2016) clearly indicate the presence of elevated weekday CO_2 emissions compared with weekend and/or holiday CO_2 emissions at two urban sites in Sakai, Japan. Cerveny and Coakley (2002) detected significantly lower CO_2 concentrations on weekends than on weekdays at Mauna Loa, which was assumed to result from anthropogenic emissions from Hawaii and nearby sources.

In this study, we present a composite 36-year record of atmospheric CO_2 measurements (1981–2016) at Mount Zugspitze, Germany (2962 m a.s.l.). The objective of this study is to achieve an improved measurement site characterization with respect to historical CO_2 data in terms of diurnal and weekly cycles, and to produce a consistent overall analysis of CO_2 trend and seasonality. The CO_2 measurements were performed at three locations on Mount Zugspitze: at a pedestrian tunnel (ZPT), at the summit (ZUG), and at the Schneefernerhaus (ZSF) on the southern face of the moun-

tain. In addition, CO_2 measurements were taken at the nearby lower mountain station, Wank Peak (WNK), but for a shorter time period. Short-term variations of weekly CO_2 periodicities and diurnal cycles were evaluated for Mount Zugspitze. In addition, a case study combining atmospheric CO and NO measurements and records of passenger numbers was used to examine weekday–weekend influences. Then the results for the CO_2 annual growth rates and seasonal amplitudes were studied separately via seasonal-trend decomposition and compared with CO_2 data for the comparable time period (1981–2016) at the Global Atmospheric Watch (GAW) regional observatory Schauinsland, Germany (SSL), and the GAW global observatory Mauna Loa, Hawaii (MLO), as well as the global CO_2 means calculated by the NOAA/ESRL and the World Data Centre for Greenhouse Gases (WDCGG).

2 Experimental methods and data

2.1 Measurement locations

Mount Zugspitze is located approximately 90 km southwest of Munich, Germany. The nearest major town is Garmisch-Partenkirchen (GAP; 708 m a.s.l.). Measurements of CO_2 were first performed between 1981 and 1997 at a southward-facing balcony in a pedestrian tunnel (ZPT; 47°25′ N, 10°59′ E; 2710 m a.s.l.) situated about 250 m below the summit of Mount Zugspitze, which joined the ancient summit station of the first Austrian cable car to the Schneefernerhaus (Reiter et al., 1986). The Schneefernerhaus was a hotel until 1992 when it was rebuilt into an environmental research station. From 1995 until 2001, a new set of measurements were made at a sheltered laboratory on the terrace of the summit (ZUG; 47°25′ N, 10°59′ E; 2962 m a.s.l.). These two measurement periods were performed by the Fraunhofer Institute for Atmospheric Environment Research (IMK-IFU), and, since 1995 these measurements have been carried out on behalf of the German Environmental Agency (UBA). Since 2001, to continue contributing to the GAW program, CO_2 measurements have been performed at the Environmental Research Station Schneefernerhaus (ZSF; 47°25′ N, 10°59′ E; 2656 m a.s.l.). Approximately 100 m below the Schneefernerhaus, the glacier plateau Zugspitzplatt can be reached from the valley via cable cars or cogwheel trains. The Zugspitzplatt descends eastward via a moderate to steep slope across the Knorrhütte towards the Reintalangerhütte as shown in Fig. 1 (Gantner et al., 2003).

2.2 Instrumental setup and data processing

CO_2 mole fractions were processed separately because of different measurement locations and time periods at Mount Zugspitze as described above. Information on the first time period (ZPT) was collected based on personal communication with corresponding staff, logbooks, and literature research (Reiter et al., 1986). The CO_2 measurement at ZPT
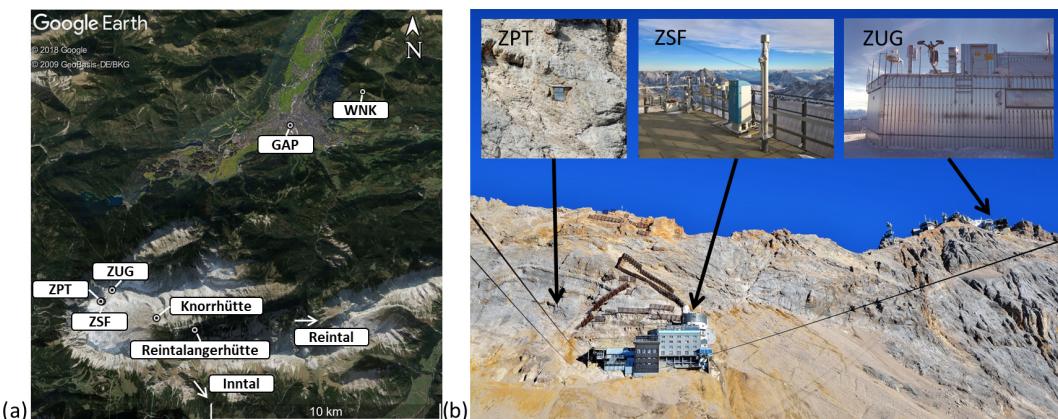
Figure 1. (a) Map showing the study area (GAP – Garmisch-Partenkirchen; WNK – Mount Wank; ZPT – pedestrian tunnel at Mount Zugspitze; ZUG – Zugspitze summit; ZSF – Zugspitze Schneefernerhaus). **(b)** A photograph showing the locations (ZPT, ZSF, and ZUG) on Mount Zugspitze at which atmospheric CO_2 measurements were performed.

was continuously performed with different instrument models used consecutively (i.e., the URAS-2, 2T, and 3G) employing the nondispersive infrared (NDIR) technique. The measured values were corrected by simultaneously measured air pressure with a hermetically sealed nitrogen-filled gas cuvette due to no flowing reference gas being used. Two commercially available working standards (310 and 380 ppm of CO_2 in N_2) were used for calibration every day at different times. The CO_2 concentration in this gas bottle was compared in short intervals with a reference standard provided by UBA which was adjusted to the Keeling standard reference scale.

At ZUG the sampling line consisted of a stainless steel tube with an inner core of borosilicate glass and a cylindrical stainless steel top cup to prevent intake of precipitation. The inlet was mounted on a small mast (approximately 4 m high) on the top of the laboratory building, which is situated on the Zugspitze summit platform (see Fig. 1b). Inside the laboratory a turbine with a fast real-time fine control ensured a constant sample inflow of $500 \, \text{L} \, \text{min}^{-1}$ of in situ air. The borosilicate glass tube (about 10 cm diameter) continued inside the laboratory, providing a number of outlets from which the instruments could get the sample air for their own analyses. The measurement and calibration were performed with a URAS-3G device and an Ansyco mixing box. The mixing controller allowed automatic switching for up to four calibration gases and sampling air by a self-written calibration routine using Testpoint software. The linear two-point calibration enveloping the actual ambient values with low and high CO_2 concentrations was taken every 25th hour. Every 6 months the working standards were checked and readjusted, when required, according to the standard reference scale using intercomparison measurements with the station standards.

At ZSF the same construction principle was applied for atmospheric sampling. There, the mast height is about 2.5 m

above the pavement of the research terrace on the fifth floor at an altitude of 2670 m a.s.l. Measurements of CO_2 at Schneefernerhaus continued thereafter until the present with a modified HP 6890 using a gas chromatograph (GC), with an intermediate upgrade in 2008 (Bader, 2001; Hammer et al., 2008; Müller, 2009). In 2012 and 2013, because of an instrumental failure of the GC, CO_2 data were recorded with a cavity ring-down spectrometer (CRDS; Picarro EnviroSense 3000i) connected to the same air inlet, which had been installed in parallel since 2011. The GC calibrations were carried out at 15 min intervals using working standards (near-ambient), which had been calibrated with station standards from the GAW Central Calibration Laboratory (CCL) operated by the NOAA/ESRL Global Monitoring Division. The GC data acquisition system (see Supplement Fig. S1) produced a calibration value every 15 min and two values from the sampled air based on one chromatogram every 5 min. For continuous quality assurance the GC was checked daily for flows, retention times, gas pressures, and the structure of chromatograms. Calibration factors and metadata were used to convert raw data into the final data product. Invalid and unrepresentative data due to local influences were flagged according to a logged list of local pollution from working activities in the research station. The measurement quality was controlled by comparison with simultaneous measurements of identical gas (CRDS) or with measurements of other trace substances and meteorological data, and additional support from station logbooks and checklists. The data were flagged according to quality control results. In principle, the acquisition system stores all measured data (flagged or not) and never discards them. Drifts in the working standards were controlled by a second target (measured approximately 25 times per day) and a regular 2-month intercomparison between the working standard and NOAA station standards, performing corrections as needed. Calibration for CRDS was performed automatically, with three different concentrations

every 12 h. Until 2013 the calibrations were performed automatically every 24 h with one concentration, very close to the ambient value. Every 2 months the concentrations were rechecked according to the station reference standards.

Additional atmospheric CO_2 measurements throughout the GAP area were performed between 1978 and 1996 at Mount Wank summit (WNK; 47°31′ N, 11°09′ E; 1780 m a.s.l.) using a URAS-2T instrument. Wank Observatory is located in an alpine grassland just above the tree line (Reiter et al., 1986; Slemr and Scheel, 1998). Detailed information on the CO_2 measurements at Schauinsland (SSL; 47°55′ N, 7°54′ E; 1205 m a.s.l.) and Mauna Loa, Hawaii (MLO; 19°28′ N, 155°35′ W; 3397 m a.s.l.), which we use to compare the results of this study with, can be found in Schmidt et al. (2003) for SSL and Thoning et al. (1989) for MLO. The CO_2 data from these measurement sites and from Mount Zugspitze locations were considered as validated data set (Level 2: calibrated, screened, and artefacts and outliers removed), without any further data processing prior to the selection of representative data. The different instruments and calibration scales used at each location are summarized in Table 1.

2.3 Offset adjustment

According to NOAA CMDL (http://ds.data.jma.go.jp/wcc/co2/co2_scale.html; last access: 23 January 2019), no significant offsets are documented between the calibration scales WMO X74 and WMO X85 and the current WMO mole fraction scale. However, for the 3-year parallel CO_2 measurements at ZPT and ZUG (1995–1997), clear offsets of -5.8 ± 0.4 ppm ($CO_{2, ZPT}$ minus $CO_{2, ZUG}$, 1 SD) were observed. The major reason for this bias is assumed to be the pressure-broadening effect in the gas analyzers used and the different gas mixtures used in the standards (Table 1), CO_2/N_2 vs. CO_2/air, the so-called "carrier gas correction" (CGC) (Bischof, 1975; Pearman and Garratt, 1975). It is known from previous studies that the measured CO_2 concentration, when using CO_2/N_2 mixtures as reference, is usually underestimated by several parts per million for the URAS instruments, and such offsets vary from different types of analyzers (Pearman, 1977; Manning and Pohl; 1986). The carrier gas effect varies even between the same type of analyzer as well as with replacement of parts of the analyzer (Griffith et al., 1982; Kirk Thoning, personal communication, 1 August 2018). Since we have insufficient information to determine a physically derived correction to the ZPT CO_2 data, an offset adjustment was made for further analyses based on the offsets in data computed in the overlapping years. A single correction factor

$$G = 0.956 + 0.00017 \cdot C_{ZPT} \tag{1}$$

was applied to the ZPT data, where C_{ZPT} denotes the CO_2 concentrations at ZPT. Because of the same calibration mixtures, an additional adjustment was applied to the CO_2 con-

centrations at WNK by calculating the CO_2 differences between ZPT and WNK. A detailed description on the offset adjustment of CGC with potential errors is given in the Supplement. Two similar CGCs by Manning and Pohl (1986) at Baring Head, New Zealand, and Cundari et al. (1990) at Mt. Cimone, Italy, were comparable in magnitude to our offset adjustment.

On the other hand, there were 9 consecutive months, from April to December 2001, of parallel atmospheric CO_2 measurements at both ZUG and ZSF, based on which an intercomparison between the two series was made. The offset between these two records attained an average of 0.1 ± 0.4 ppm ($CO_{2, ZUG}$ minus $CO_{2, ZSF}$, 1 SD), which fulfills the requirement of the GAW data quality objective (DQO; ± 0.1 ppm) for atmospheric CO_2 in the Northern Hemisphere. Therefore, no adjustments regarding this offset were applied to the data sets.

In this study, we took CO_2 measurements during the corresponding time intervals at ZPT (1981–1994), ZUG (1995–2001), and ZSF (2002–2016) to assemble a composite time series for Mount Zugspitze over 36 years. Nevertheless, we always treat measurements from each location separately for further analyses. At WNK, as well as at SSL and MLO, we used measured CO_2 data starting from 1981 for time consistency with measurements at Mount Zugspitze.

2.4 ADVS data selection

Adaptive diurnal minimum variation selection (ADVS), a recently published, novel statistical data selection strategy, was used to ensure that the data were clean and consistent with respect to the state of a locally unaffected lower free troposphere at the measurement sites (Yuan et al., 2018). ADVS, which was originally designed to characterize mountainous sites, selects data based on diurnal patterns, with the aim of selecting optimal data that can be considered representative of the lower free troposphere. To achieve this, variations in the mean diurnal CO_2 were first evaluated and a time window was selected based on minimal data variability around midnight, at which point data selection began. The data outside the starting time window were examined on a daily basis both forward and backward in time for the day under consideration, by applying an adaptive threshold criterion. The selected data represent background CO_2 levels at the different measurement sites.

ADVS data selection was applied to all CO_2 records based on the same threshold parameters, followed by examining the starting time window and calculating the percentages of the ADVS-selected data. Figure 2a shows the CO_2 time series before and after ADVS data selection. We also evaluated the starting time windows resulting from ADVS data selection with the detrended mean diurnal cycles as described in Yuan et al. (2018) for each measurement site in Fig. 2b. The number of ADVS-selected data is summarized as percentage per

Table 1. Detailed description of atmospheric CO_2 measurement techniques (NDIR is the nondispersive infrared, GC is gas chromatography, and CRDS is cavity ring-down spectroscopy). At ZSF, CO_2 data from GC measurements were not available from 2012 to 2013 due to an instrumental failure; thus data from CRDS measurements were used in these 2 years for this study. However, CRDS measurements were performed in parallel from the same air inlet from 2011.

ID	Time period	Instrument (analytical method)	Scale	Calibration gas
ZPT	1981–1997	1981–1984: Hartmann & Braun URAS 2 (NDIR) 1985–1988: Hartmann & Braun URAS 2T (NDIR) 1989–1997: Hartmann & Braun URAS 3G (NDIR)	WMO X74 scale	CO_2 in N_2
ZUG	1995–2001	Hartmann & Braun URAS 3G (NDIR)	WMO X85 scale	CO_2 in natural air
ZSF	2001–2016	2001–2016: Hewlett Packard Modified HP 6890 Chem. station (GC) 2012–2013: Picarro EnviroSense 3000i (CRDS)	WMO X2007 scale	CO_2 in natural air
WNK	1981–1996	Hartmann & Braun URAS 2T (NDIR)	WMO X74 scale	CO_2 in N_2
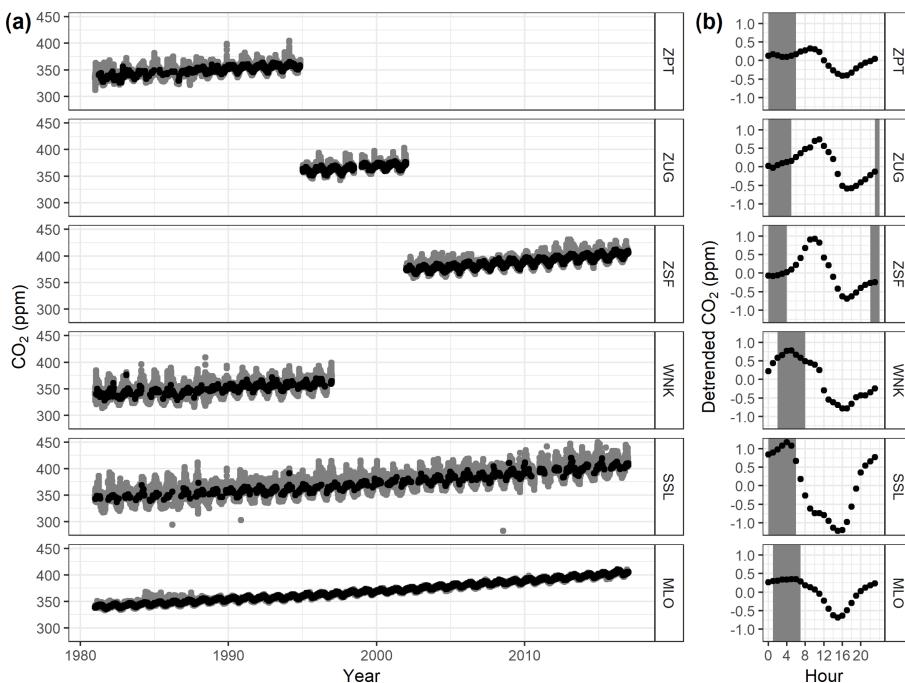
Figure 2. (a) Time series plot of 30-min averaged CO_2 concentrations measured at Mount Zugspitze (ZPT, ZUG, and ZSF) and Wank (WNK), and hourly averaged CO_2 concentrations measured at Schauinsland (SSL) and Mauna Loa (MLO) with ADVS selection. Grey and black colors are used for the unselected and selected results. **(b)** Detrended mean diurnal cycles with starting time windows (in grey) for ADVS data selection.

hour in the total number of all CO_2 data in Fig. 3. A detailed description and discussion is given in Sect. 3.1.

2.5 Mean symmetrized residual

Weekly periodicity was calculated using the mean symmetrized residual (MSR) method, which was originally applied to atmospheric CO_2 data (Cerveny and Coakley, 2002). The MSR method focuses on variations in mean values for the days of the week. Daily deviations from the 7-day (consecutive) averages are calculated without ADVS selection to account for the most likely emission cycles. Then, the MSR values are derived by averaging the differences for each sin-

gle day. Additionally, only the MSR values with no data gaps in all the seven differences are considered as valid. Finally, all the MSR values are aggregated into overall mean values for each day of the week. In addition, the MSR values are standardized so that the sum of all the seven values is equal to 0 (Cerveny and Coakley, 2002).

2.6 STL decomposition

The seasonal-trend decomposition technique (STL) was applied to decompose the CO_2 time series into trend, seasonal, and remainder components individually (Cleveland et al., 1983, 1990), which, in previous studies, has been

a commonly applied method (e.g., Stephens et al., 2013; Hernández-Paniagua et al., 2015). Locally weighted polynomial regressions were iteratively fitted to all monthly values in both an outer and an inner loop. According to Cleveland et al. (1990) and Pickers and Manning (2015), we set the trend and seasonal smoothing parameters to 25 and 5, respectively. The CO$_2$ time series at each site or location were aggregated into monthly averages and, then, decomposed using STL. Missing monthly values were substituted using spline interpolation.

To study the trend and seasonality, we firstly intended to apply STL decomposition to the ADVS-selected time series. However, due to multiple occurrences of consecutively missing values in the ADVS-selected monthly averages, especially for measurement sites at lower elevations (WNK and SSL), it was more practical to use the original CO$_2$ time series without ADVS data selection for STL decomposition, to preserve time series continuity (Pickers and Manning, 2015). There is one missing 6-month time interval at ZUG in 1998 (July to December). Thus STL was performed separately for the time periods before (January 1995–June 1998) and after (January 1999–December 2001) the gap. Nevertheless, we still applied STL decomposition to the ADVS-selected data sets from Mount Zugspitze and Mauna Loa, since these selected time series were applicable. At ZPT, due to larger time gaps of missing data at the beginning (1981 and 1982) of the ADVS-selected data set, the ADVS-selected and STL-decomposed results were only studied starting from 1983. Individual figures of each STL-decomposed component at all stations can be found in the Supplement.

For annual growth rates we did not include the WNK time series due to shorter time periods of available data. Monthly trend components were first aggregated into annual mean values. Then, the annual CO$_2$ growth rates were calculated as the difference between the CO$_2$ value of the current year and the value from the previous year (Jones and Cox, 2005). The mean seasonal cycle was aggregated directly from the monthly seasonal components by month. To observe potential deviations on the regional and global scale, we compared the trend and seasonality derived from the STL-decomposed components at Zugspitze with other measurement sites. We included the globally averaged marine surface monthly mean data from NOAA (https://www.esrl.noaa.gov/gmd/ccgg/trends/; last access: 23 January 2019) and data for the global mean mole fractions from WDCGG (WMO Greenhouse Gas Bulletin, 2018) as references, and processed these data based on the identical STL decomposition routine. All the statistical analyses described above (including ADVS, MSR, and STL) were performed in the R environment (R Core Team, 2018).

3 Results and discussion

3.1 ADVS selection and diurnal variation

The resulting ADVS-selected CO$_2$ data showed a clear linkage of the percentage of selected data and the altitude of the measurement site. Among the continental stations, the percentage increased with altitude. A lower percentage indicates higher data variability due to lower elevation and proximity to local sources and sinks. At Schauinsland, the percentage of CO$_2$ data by the ADVS selection was 6.3 %, while the percentages at Mount Zugspitze reached 9.9 % (ZPT), 19.5 % (ZUG), and 13.6 % (ZSF), respectively. A moderate percentage of 6.3 % was also derived at Mount Wank. However, regarding the elevated mountain station Mauna Loa on the island of Hawaii, a much higher percentage (40.0 %) of CO$_2$ data was selected using ADVS as being representative of its background concentration, mainly due to the very limited nearby anthropogenic sources as well as mostly clean, well-mixed air arriving there. A similar result for an island mountain station can be found in Yuan et al. (2018), in which a percentage of 36.2 % was computed for the CO$_2$ measurements at Izaña station on the island of Tenerife (28°19′ N, 16°30′ E; 2373 m a.s.l.). This can also be explained by the detrended mean diurnal cycles shown in Figs. 2b and 3. The mean diurnal cycle at MLO only exhibits a clear trough during daytime, especially starting from 12:00 local time (LT), which is believed to be influenced by the vegetation activity (photosynthesis) in the surroundings. The same effect can be seen at WNK and SSL, but with larger magnitudes and earlier occurrences of the minima because of their lower locations closer to CO$_2$ sinks. In contrast, at these two sites the CO$_2$ maxima in the diurnal cycles were not as clearly noticeable as at Mount Zugspitze due to anthropogenic sources and high biogenic respiration. At the three locations on Mount Zugspitze, the CO$_2$ peaks in the mean diurnal cycles are driven by the late-morning convective upslope wind, which was relatively obvious at both ZUG and ZSF. However, from the perspective of data selection, a significantly higher percentage of CO$_2$ data was selected at ZSF compared with ZPT, although there is only a small difference in altitude of around only 70 m. This proves that ZSF is capable of capturing more background conditions than ZPT during the day. Nevertheless, based on the starting time window computed for ADVS selection, we found that, in general, most stations exhibited similar starting time windows beginning around midnight, and the ADVS data selection was applied systematically by including more data around these hours (see Fig. 3), which confirmed our assumption of background conditions during midnight for the ADVS data selection (Yuan et al., 2018).

3.2 Weekly periodicity

For a better characterization of the differences among the measurement locations at Mount Zugspitze, the mean CO$_2$
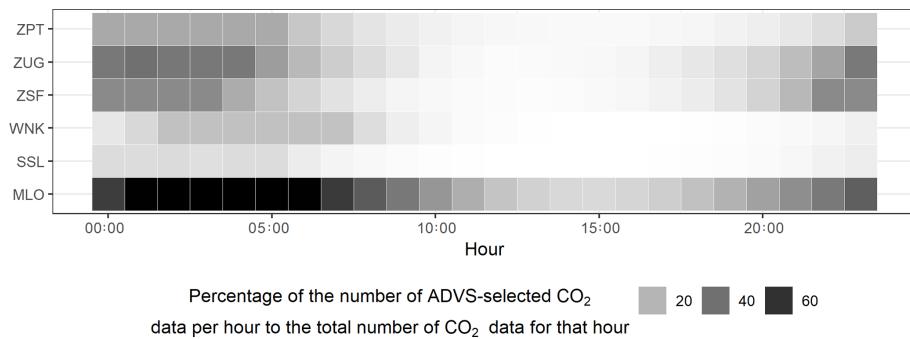
Figure 3. Frequency of the percentages of the number of ADVS-selected CO_2 data for each hour (0 to 23) in the total number of CO_2 data for that hour as shown in greyscale.
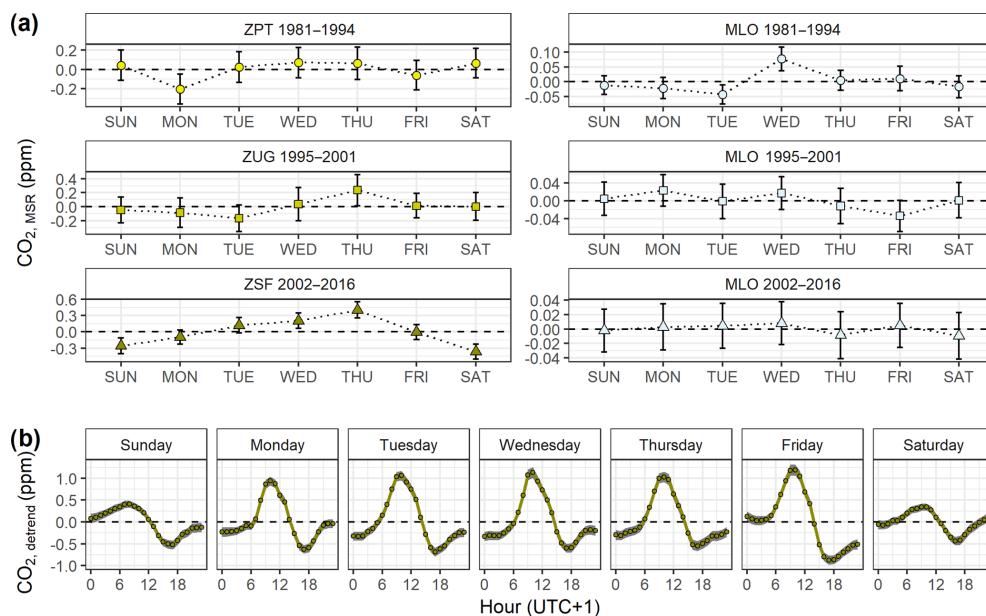

Figure 4. (a) Mean MSR CO_2 values at Mount Zugspitze and MLO as a function of the day of the week. Mean MSR values are adjusted such that they sum to 0. **(b)** Detrended mean CO_2 diurnal cycles at ZSF by day of the week from 2002 to 2016. Uncertainties at the 95 % confidence interval are shown by the shaded areas.

weekly cycles were analyzed as a function of mean MSR values (see Fig. 4a). The mean MSR values at the MLO for the corresponding time intervals were also calculated. Most weekly cycles exhibited no clear peaks or patterns for both sites. However, the magnitude of MSR data variability is mostly higher at Zugspitze, with a maximum on Thursdays. The only significant weekday–weekend difference is observed at ZSF in terms of the 95 % confidence interval, which shows weekly maxima and weekly minima on Thursday and Saturday, respectively (peak-to-trough difference: 0.76 ppm). Gilge et al. (2010) observed similar phenomena when studying O_3 and NO_2 concentrations at Alpine mountain stations, including Zugspitze. Clear weekly cycles, with enhanced O_3 levels on working days, were observed at ZSF in summer, with weekly maxima and minima on Thursdays and Sundays, respectively. For NO_2, maximum mixing ratios

on working days and minimum ratios on Sundays at neighboring stations were observed, generally suggesting an anthropogenic impact at all elevations.

We obtained more insights into the weekly CO_2 cycle at Mount Zugspitze by comparing the mean diurnal cycles of weekdays and weekends (see Fig. 4b). Detrended mean diurnal cycles at ZSF, from Sunday to Saturday, were calculated by subtracting the daily averages from the daily data between 2002 and 2016. In the morning around 09:00 to 10:00 LT the CO_2 levels at ZSF are higher on weekdays than weekends, while CO_2 diurnal patterns during the rest of the week are relatively stable. Such weekly cycles are not observable at ZPT and ZUG, nor at WNK and SSL (see Fig. S18). At ZPT, there are fewer variations in the diurnal cycle compared to ZSF, indicating that this location does not receive the effect of regular local anthropogenic working activities and hence it

is more representative of lower free tropospheric conditions regarding this aspect. The weekday–weekend differences at ZSF are possibly due to local working patterns, whereas the absence of this pattern at lower sites may indicate influences from a more regional reservoir. In fact, ZSF is closed on the weekends and, thus, is influenced by less immediate anthropogenic activities.

3.3 Case study on atmospheric CO and NO and passenger numbers at Zugspitze

To study the potential sources and sinks for such weekday–weekend differences in the CO_2 diurnal cycles at ZSF further, we analyzed atmospheric CO and NO data at ZSF and the daily combined number of cable car and train passengers to Zugspitzplatt and to the Zugspitze summit in 2016. Atmospheric CO and NO are known to be good indicators of local anthropogenic influences due to highly variable short-term signals and are thus helpful to identify potential CO_2 sources (Tsutsumi et al., 2006; Sirignano et al., 2010; Wang et al., 2010; Liu et al., 2016). In this study, we used atmospheric NO due to its short lifetime based on rapid atmospheric NO_2 formation with resulting altitude-dependent O_3 surplus, indicating the presence of sources at closer distances. The CO and NO data shown in Fig. 5 include data that were flagged during data processing because for the delivery to GAW World Data Centres the logged and recognized work-dependent concentration peaks are flagged. A clear weekday–weekend difference is observed for both CO and NO. Only weekdays are characterized by multiple short-term atmospheric CO events and higher atmospheric NO peaks during the daytime (mostly around 09:00 LT), which fits perfectly with daytime peaks in CO_2 diurnal cycles. A general fluctuating pattern in NO throughout the week is thought to originate from heating of the Zugspitzplatt and changing work with combustion engines. On the other hand, the daily number of passengers at Zugspitze (see Fig. 5c) shows a clear weekday–weekend pattern, with a higher number of passengers on the weekends. However, increased numbers of passengers on the weekends do not correspond to higher levels of CO and CO_2, indicating that measured CO_2 levels are not significantly influenced by tourist activities nearby. Instead, it is more likely that anthropogenic working activities are the main driver of weekly periodicity.

3.4 Trend

Based on the STL-decomposed results, the mean annual growth rate of the 36-year composite record at Mount Zugspitze from the three measurement locations is 1.8 ± 0.4 ppm yr^{-1}, which is consistent with the SSL (1.8 ± 0.4 ppm yr^{-1}), MLO (1.8 ± 0.2 ppm yr^{-1}), and global means (NOAA: 1.8 ± 0.2 ppm yr^{-1}; WDCGG: 1.8 ± 0.2 ppm yr^{-1}). The mean annual growth rates from the ADVS-selected data sets at Mount Zugspitze and Mauna Loa also result in the

identical value of 1.8 ppm yr^{-1}. Then, we divided the entire time period (1981–2016) into three time blocks, corresponding to the different locations at Mount Zugspitze, in order to observe potential differences with respect to other sites separately (see Table 2). The results show good agreement of each location on Mount Zugspitze with other measurement sites (also for the ADVS-selected results) as well as a clearly increasing trend of the annual growth rates over these three time blocks. Only the mean annual growth rate between 1995 and 2001 at ZUG is obviously lower than at the other sites. This can be explained by the missing monthly values in 1998, and thus in turn the annual growth rates of 1998 and 1999 were left out for the average. However, the annual growth rates of these 2 years reached anomalous peaks at most sites (see details later in Sect. 3.6). Möller (2017) also mentioned that 1981 to 1992 growth rates at both German stations and MLO were identical.

3.5 Seasonality

For the overall seasonality, Fig. 6 presents the mean seasonal cycles for the STL-decomposed seasonal components. We observed similar patterns in the SSL and WNK seasonal cycles, with mean peak-to-trough amplitudes of 15.9 ± 1.0 and 15.9 ± 1.5 ppm, respectively. The composite data set at Mount Zugspitze results in a lower amplitude (12.4 ± 0.6 ppm), but still exhibits a similar seasonality influenced by active biogenic processes (mainly photosynthesis) in summer compared with SSL and WNK (Dettinger and Ghil, 1998). As vegetation grows with rising temperatures (approaching summer), CO_2 levels decrease due to more and more intense photosynthetic activities till a minimum in August. In addition, with rising temperatures, locally influenced air masses reach Mount Zugspitze more often due to "Alpine pumping" (Carnuth et al., 2002; Winkler et al., 2006). As such, air sampled in summer is more frequently mixed with air from lower levels, which is characterized by lower CO_2 concentrations, intensifying the August minimum. Anthropogenic activities and plant respiration dominate the increases in concentration in the winter (January to April). This influence appears to be stronger at SSL and WNK than at Mount Zugspitze. Lower levels of CO_2 and a 1-month delay, from February to March, of the seasonal maximum at Mount Zugspitze are in agreement with the expectation of thermally driven orographic processes that drive the upward transport of CO_2 from local sources, as well as limited human access to Mount Zugspitze and the prevailing absence of biogenic activities at such high elevations. Regarding the resulting seasonal cycles based on ADVS-selected Zugspitze data sets, similar patterns were observed but with a lower amplitude (10.5 ± 0.5 ppm) as well as a 2-month shift of the seasonal maximum to April.

The Mauna Loa CO_2 record is characterized by a seasonal maximum in May and a minimum in September, with a peak-to-trough amplitude of 6.8 ± 0.1 ppm, which agrees with observations from Dettinger and Ghil (1998) and Lint-
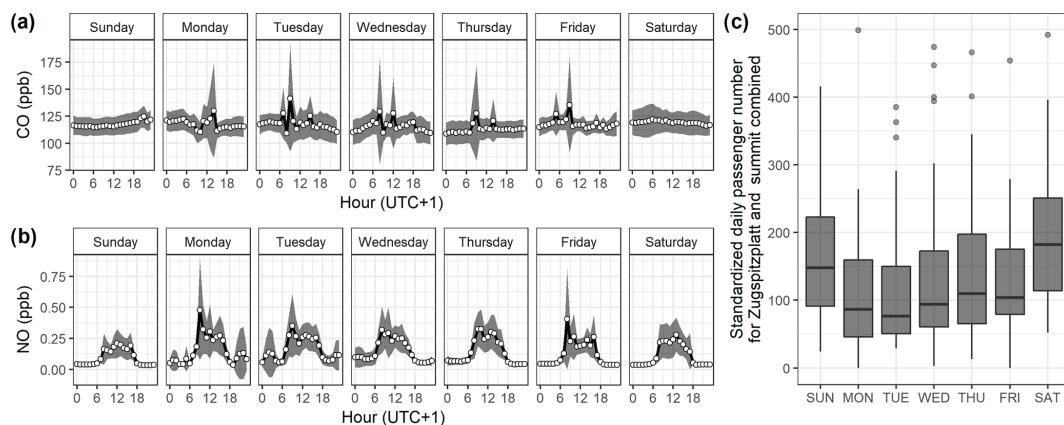
Figure 5. Mean diurnal plots at ZSF during 2016 by day of the week for **(a)** CO and **(b)** NO, and **(c)** the standardized daily passenger number at the Zugspitzplatt and Zugspitze summit combined.

Table 2. Mean annual CO_2 growth rates in $\mathrm{ppm\,yr^{-1}}$ at the 95 % confidence interval based on three time blocks for all measurement sites/locations studied (SSL – Schauinsland; WNK – Mount Wank; ZPT – pedestrian tunnel at Mount Zugspitze; ZUG – Zugspitze summit; ZSF – Zugspitze Schneefernerhaus; MLO – Mauna Loa; WDCGG and NOAA – global means). ADVS means the data were selected using the ADVS method. This comparison refers to data from all years including the corresponding time period for all stations. Measurement sites or locations where data are not available for calculating the corresponding time blocks are shown by "–".

Time block	SSL	WNK	ZPT	ZPT ADVS	ZUG	ZUG ADVS	ZSF	ZSF ADVS	MLO	MLO ADVS	WDCGG	NOAA
1981–1994	1.5 ± 0.5	1.4 ± 1.1	1.5 ± 0.8	1.5 ± 1.4	–	–	–	–	1.4 ± 0.3	1.4 ± 0.3	1.4 ± 0.4	1.4 ± 0.3
1995–2001	1.7 ± 1.1	–	–	–	1.3 ± 0.8	1.5 ± 0.5	–	–	1.8 ± 0.5	1.8 ± 0.5	1.8 ± 0.4	1.7 ± 0.5
2002–2016	2.2 ± 0.7	–	–	–	–	–	2.2 ± 0.4	2.2 ± 0.4	2.2 ± 0.2	2.2 ± 0.2	2.2 ± 0.2	2.2 ± 0.2
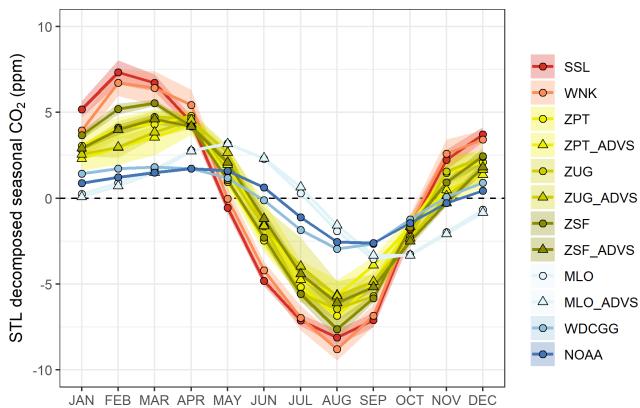
Figure 6. Mean CO_2 seasonal cycles from the STL seasonal component at each measurement site or location. Uncertainties at the 95 % confidence interval are shown by the shaded areas with corresponding colors.

ner et al. (2006). The ADVS-selected results for MLO also show a similar pattern, with a lower amplitude of 6.6 ± 0.1 ppm. Global means exhibited the lowest seasonal amplitudes, 4.4 ± 0.1 ppm (NOAA) and 4.8 ± 0.0 ppm (WDCGG). Compared with WDCGG, the NOAA global mean better fits the seasonal cycle of MLO supporting the presence of a typ-

ical marine boundary layer (MBL) condition for the levels of background CO_2 in the atmosphere. On the other hand, the WDCGG global mean includes continental characteristics for its calculation, thus exhibiting a slightly more continental signature which can be equally seen in the seasonal cycles at continental sites, such as Mount Zugspitze. April and October appear to be the important months that indicate the switch of either CO_2 source to sinks or vice versa for the continent.

We then examine in more detail the seasonal cycles at ZPT, ZUG, and ZSF. Despite the close proximity, there are differences in their seasonal amplitudes (ZPT: 11.9 ± 1.2 ppm; ZUG: 11.2 ± 1.0 ppm; ZSF: 13.3 ± 0.7 ppm). Good agreement is shown between CO_2 seasonal cycles from April to June and from October to December. However, significantly higher levels of CO_2 were evident at ZSF from January to March as well as lower levels from July to September. After data selection with lower seasonal amplitudes of 10.3 ± 1.3 (ZPT_ADVS), 10.3 ± 1.2 (ZUG_ADVS), and 10.9 ± 0.6 ppm (ZSF_ADVS), similar differences of the CO_2 levels in the seasonal cycles could be observed. These results indicate that factors such as elevation and measurement surroundings strongly determine the air-mass composition via local vertical transport. The amount of air-mass transport via orographic lifting affects the three locations differently. The

lower elevation station, ZSF, apparently captures more mixed air masses due to a daytime up-valley flow along the Reintal (Gantner et al., 2003) as well as a slightly southeastern flow from the Inntal (see Fig. 1) that is less frequent for the higher locations (ZPT or ZUG). In addition, comparably postponed seasonal maxima at ZUG and ZPT from March to April show delayed onset of convective upwind air-mass transport and changing planetary boundary layer (PBL) compositions. On the other hand, these differences in the seasonal amplitudes (even though not significant at the 95 % confidence interval) might be influenced by a potential trend in the seasonal amplitude over time. Such increasing trends of the seasonal CO_2 amplitudes (i.e., +0.32 % yr^{-1} at Mauna Loa and +0.60 % yr^{-1} at Utqiaġvik, formerly Barrow, Alaska) were studied in Graven et al. (2013), indicating an enhanced interaction between the biospheric and atmospheric CO_2 across the Northern Hemisphere.

3.6 Interannual variation

To study the interannual variability, we focused on the percentages of ADVS selection, the growth rates, and the seasonal amplitudes. The annual percentages from ADVS data selection are shown for years without missing monthly averages (see Fig. 7a). An exceptionally high percentage at Zugspitze in 2000 resulted from careful and intensive filtering of the original CO_2 data. The total number of original validated 30 min data points in 2000 is only 4634, while the number of data for other years ranges from 8754 to 15 339 (except for 1998, with only 6-month data, the total number of 30 min CO_2 data is 6441). As described in the previous section, the annual growth rates are plotted in Fig. 7b. The annual CO_2 seasonal amplitudes are calculated as the difference between the yearly maximum and minimum monthly CO_2 values from the STL-decomposed seasonal components (see Fig. 7c).

Focusing on the annual percentages from ADVS-selected representative data after 1990, we calculated the mean annual percentages at Mount Zugspitze locations, for the time periods between 1990 and 2001 (2000 was not included for ZUG) and 2002 and 2016. We observe significantly higher percentages at ZPT and ZUG (18.5 ± 2.4 %) than at ZSF (13.6±1.1 %) at the 95 % confidence interval. These percentages are different from SSL (4.2±0.5 % vs. 4.2±0.6 %) and MLO (43.5 ± 1.4 % vs. 42.1 ± 1.6 %). A likely explanation is that there are systematically different air-mass transport characteristics reaching each of these locations. Higher percentages at ZPT and ZUG indicate that these locations are capable of capturing more air masses that have traveled over long distances along the mountains. These air masses trap air that ascends from many Alpine valleys, but also from remote source regions up to the intercontinental scale (Trickl et al., 2003; Huntrieser et al., 2005). On the other hand, ZSF is dominated by mixing air masses that have traveled along the Zugspitzplatt area, which contain higher levels of

CO_2 due to daily, local anthropogenic sources during winter and convective upwind transport during seasons without snow cover that are characterized by lower concentrations of CO_2 at lower altitudes. Such patterns in the data are also evident in the annual growth rates and seasonal amplitudes. The overall patterns at Mount Zugspitze agree with SSL and WNK. However, SSL and WNK exhibit more variation in the annual growth rates and higher seasonal amplitude levels (see Fig. 7b and c). In addition, slightly higher seasonal amplitudes for the WDCGG global mean compared with the NOAA one can be explained by the WDCGG global mean calculation method, which includes more continental stations (WMO Greenhouse Gas Bulletin, 2018).

Anomalies in the annual growth rates are frequently observed, which are possibly explained by climatic influences such as the El Niño–Southern Oscillation (ENSO), volcanic activity, and extreme weather conditions (Keeling et al., 1995; Jones and Cox, 2001; Francey et al., 2010; Keenan et al., 2016). One of the largest positive annual growth rate anomalies occurred in 1998 and is clearly seen in all the records (aside from ZUG with missing values), which is attributed to a strong El Niño event (Watanabe et al., 2000; Jones and Cox, 2005). Similar signals are found in 1988, especially at MLO and in global means. Such anomalies are more clearly observed in the global and seaside time series. Regarding continental sites, interannual signals may be hidden by more intense land influences rather than global effects. Moreover, positive consecutive anomalies between 2002 and 2003 are clearly observed at ZSF and SSL, which are potentially due to anomalous climatic conditions, such as the dry European summer in 2003 that led to an increasing number of forest fires. These events are also observable in the MLO and global means but at a smaller scale (Jones and Cox, 2005). At all German sites, clear negative anomalies, due to violent eruptions of the El Chichón and Mt. Pinatubo volcanoes and the subsequent volcanic-induced surface cooling effect are observed after stratospheric aerosol maxima above Garmisch-Partenkirchen in 1983 and 1992, respectively (Lucht et al., 2002; Frölicher et al., 2011, 2013; Trickl et al., 2013). This effect is only slightly visible in the MLO and global means despite the fact that volcanic aerosols spread over the entire globe.

However, the reasons for some anomalies are still unclear. These include the negative anomalies during 1985 and 1986 at all Germans sites. Certain anomalies in the annual percentages and seasonal amplitudes also derive from extremely low ADVS selection percentages beginning in 1984 and continuing until 1990, with peaks in seasonal amplitudes between 1985 and 1986. This is the reason why we calculated the mean annual ADVS selection percentage beginning at 1990. We assume that local influences mask similar physical mechanisms at the sites. However, annual percentages at the MLO also have similar characteristics. Therefore, it is still unclear what triggers such distinct interannual data variability across measurement sites. Another clear negative annual
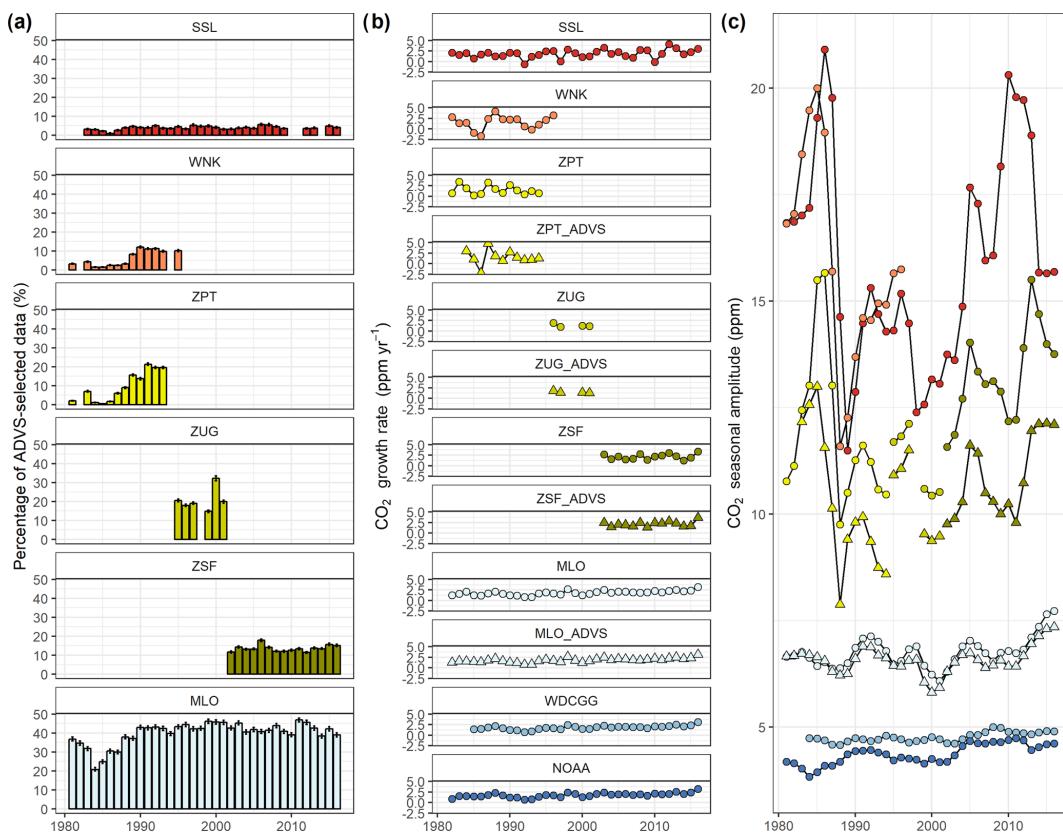
Figure 7. (a) Annual ADVS-selected percentages. **(b)** Annual CO_2 growth rates and global means from the NOAA and the WDCGG. The calculated growth rates are shown at the beginning of the year. Since the time period starts in 1981, the values of growth rates start in 1982. WDCGG data are only available starting in 1984. **(c)** Annual CO_2 seasonal amplitudes.

growth rate anomaly occurred in 2014 across all sites. Such anomalies still require further investigation, but are beyond the scope of this study.

4   Conclusions

In this study, we presented a time series analysis of a 36-year composite CO_2 measurement record at Mount Zugspitze in Germany, together with a thorough study of the weekly periodicity combined with diurnal cycles. Even though it is challenging to quantify local sources and sinks, this study shows that it is possible to gain information on variation in this regard. Compared with the GAW regional observatories at Schauinsland and Wank Peak, as well as the GAW global observatory at Mauna Loa, Mount Zugspitze proves to be a highly suitable site for monitoring the background levels of air components using proper data selection procedures. The long-term trend at Zugspitze agrees well with that at Mauna Loa and global means. The seasonality and short-term variations show similar patterns, but are considerably less influenced by local to regional mechanisms than the lower elevation stations at Schauinsland and Wank Peak. Interannual variations also correlate well with anomalous global events.

However, several anomalies still exist across most stations that lack clear explanations. These anomalies require further investigation, possibly by analyzing correlations between extreme events and historical meteorological or hydrological data. Finally, we conclude that, at Zugspitze, we cannot neglect local to regional influences. Regarding the seasonal amplitude, Mount Zugspitze is significantly more influenced by biogenic activity, mostly in the summer, compared with Mauna Loa and global means. On the other hand, the weekly periodicity analysis provides a clear picture of local CO_2 sources that potentially result from human working activities, especially at ZSF. Overall, this study provides detailed insights into long-term atmospheric CO_2 measurements, as well as site characteristics at Mount Zugspitze. We propose the application of this type of analysis as a systematic tool for the physical and quantitative classification of stations with respect to their lower free tropospheric representativeness. As an additional component in this analysis, weekly periodicity can be used to analyze anthropogenic influences. The systematic application of this approach to larger continental or global regions can serve as a basis for more quantitative analyses of global greenhouse gases trends such as CO_2. Based on the physical foundation of the methodology pre-

sented here, we suggest that these techniques can be applied to other greenhouse gases such as SF$_6$, CH$_4$, and aerosols.

Author contributions. YY, LR, HP, and AM designed the study and YY performed the data analyses with help from LR and HP for the data processing and code validation. Atmospheric measurement data were collected, preprocessed, and provided by LR, TT, CC, RS, and FM. Information about data quality assurance and measurement site was provided by LR. YY prepared the manuscript with contributions from all co-authors.

References

Bader, J.: Aufbau und Betrieb eines automatisierten Gaschromatographen HP 6890 zur kontinuierlichen Messung von CO$_2$, CH$_4$, N$_2$O und SF$_6$, Universität Heidelberg, 2001.

Beardsmore, D. J. and Pearman, G. I.: Atmospheric carbon dioxide measurements in the Australian region: Data from surface observatories, Tellus B, 39, 42–66, https://doi.org/10.1111/j.1600-0889.1987.tb00269.x, 1987.

Bischof, W.: The influence of the carrier gas on the infrared gas analysis of atmospheric CO$_2$, Tellus, 27, 59–61, https://doi.org/10.3402/tellusa.v27i1.9884, 1975.

Bousquet, P., Gaudry, A., Ciais, P., Kazan, V., Monfray, P., Simmonds, P. G., Jennings, S. G., and O'Connor, T. C.: Atmospheric CO$_2$ concentration variations recorded at Mace Head, Ireland, from 1992 to 1994, Phys. Chem. Earth, 21, 477–481, https://doi.org/10.1016/S0079-1946(97)81145-7, 1996.

Carnuth, W. and Trickl, T.: Transport studies with the IFU three-wavelength aerosol lidar during the VOTALP Mesolcina experiment, Atmos. Environ., 34, 1425–1434, https://doi.org/10.1016/S1352-2310(99)00423-9, 2000.

Carnuth, W., Kempfer, U., and Trickl, T.: Highlights of the tropospheric lidar studies at IFU within the TOR project, Tellus B, 54, 163–185, https://doi.org/10.1034/j.1600-0889.2002.00245.x, 2002.

Cerveny, R. S. and Coakley, K. J.: A weekly cycle in atmospheric carbon dioxide, Geophys. Res. Lett., 29, 15-1–15-4, https://doi.org/10.1029/2001GL013952, 2002.

Ciattaglia, L.: Interpretation of atmospheric CO$_2$ measurements at Mt. Cimone (Italy) related to wind data, J. Geophys. Res., 88, 1331, https://doi.org/10.1029/JC088iC02p01331, 1983.

Cleveland, R. B., Cleveland, W. S., McRae, J. E., and Terpenning, I.: STL: A seasonal-trend decomposition procedure based on loess, J. Off. Stat., 6, 3–73, 1990.

Cleveland, W. S., Freeny, A. E., and Graedel, T. E.: The seasonal component of atmospheric CO$_2$: Information from new approaches to the decomposition of seasonal time series, J. Geophys. Res., 88, 10934, https://doi.org/10.1029/JC088iC15p10934, 1983.

Cundari, V., Colombo, T., Papini, G., Benedicti, G., and Ciattaglia, L.: Recent improvements on atmospheric CO_2 measurements at Mt. Cimone observatory, Italy, Il Nuovo Cimento C, 13, 871–882, https://doi.org/10.1007/BF02512003, 1990.

Dettinger, M. D. and Ghil, M.: Seasonal and interannual variations of atmospheric CO_2 and climate, Tellus B, 50, 1–24, https://doi.org/10.1034/j.1600-0889.1998.00001.x, 1998.

Francey, R. J., Trudinger, C. M., van der Schoot, M., Krummel, P. B., Steele, L. P., and Langenfelds, R. L.: Differences between trends in atmospheric CO_2 and the reported trends in anthropogenic CO_2 emissions, Tellus B, 62, 316–328, https://doi.org/10.1111/j.1600-0889.2010.00472.x, 2010.

Frölicher, T. L., Joos, F., and Raible, C. C.: Sensitivity of atmospheric CO_2 and climate to explosive volcanic eruptions, Biogeosciences, 8, 2317–2339, https://doi.org/10.5194/bg-8-2317-2011, 2011.

Frölicher, T. L., Joos, F., Raible, C. C., and Sarmiento, J. L.: Atmospheric CO_2 response to volcanic eruptions: The role of ENSO, season, and variability, Global Biogeochem. Cy., 27, 239–251, https://doi.org/10.1002/gbc.20028, 2013.

Gantner, L., Hornsteiner, M., Egger, J., and Hartjenstein, G.: The diurnal circulation of Zugspitzplatt: Observations and modeling, Meteorol. Z., 12, 95–102, https://doi.org/10.1127/0941-2948/2003/0012-0095, 2003.

Gilge, S., Plass-Duelmer, C., Fricke, W., Kaiser, A., Ries, L., Buchmann, B., and Steinbacher, M.: Ozone, carbon monoxide and nitrogen oxides time series at four alpine GAW mountain stations in central Europe, Atmos. Chem. Phys., 10, 12295–12316, https://doi.org/10.5194/acp-10-12295-2010, 2010.

Graven, H. D., Keeling, R. F., Piper, S. C., Patra, P. K., Stephens, B. B., Wofsy, S. C., Welp, L. R., Sweeney, C., Tans, P. P., Kelley, J. J., Daube, B. C., Kort, E. A., Santoni, G. W., and Bent, J. D.: Enhanced seasonal exchange of CO_2 by northern ecosystems since 1960, Science, 341, 1085–1089, https://doi.org/10.1126/science.1239207, 2013.

Griffith, D. W. T., Keeling, C. D., Adams, A., Guenther, P. R., and Bacastow, R. B.: Calculations of carrier gas effects in non-dispersive infrared analyzers. II. Comparisons with experiment, Tellus, 34, 385–397, https://doi.org/10.3402/tellusa.v34i4.10825, 1982.

Hammer, S., Glatzel-Mattheier, H., Müller, L., Sabasch, M., Schmidt, M., Schmitt, S., Schönherr, C., Vogel, F., Worthy, D. E., and Levin, I.: A gas chromatographic system for high-precision quasi-continuous atmospheric measurements of CO_2, CH_4, N_2O, SF_6, CO and H_2, available at: http://www.iup.uni-heidelberg.de/institut/forschung/groups/kk/en/GC_Hammer_25_SEP_2008.pdf (last access: 23 January 2019), 2008.

Hernández-Paniagua, I. Y., Lowry, D., Clemitshaw, K. C., Fisher, R. E., France, J. L., Lanoisellé, M., Ramonet, M., and Nisbet, E. G.: Diurnal, seasonal, and annual trends in atmospheric CO_2 at southwest London during 2000–2012: Wind sector analysis and comparison with Mace Head, Ireland, Atmos. Environ., 105, 138–147, https://doi.org/10.1016/j.atmosenv.2015.01.021, 2015.

Huntrieser, H., Heland, J., Schlager, H., Forster, C., Stohl, A., Aufmhoff, H., Arnold, F., Scheel, H. E., Campana, M., Gilge, S., Eixmann, R., and Cooper, O. R.: Intercontinental air pollution transport from North America to Europe: Experimental evidence from airborne measurements and surface observations, J. Geophys. Res., 110, D01305, https://doi.org/10.1029/2004JD005045, 2005.

Jones, C. D. and Cox, P. M.: Modeling the volcanic signal in the atmospheric CO_2 record, Global Biogeochem. Cy., 15, 453–465, https://doi.org/10.1029/2000GB001281, 2001.

Jones, C. D. and Cox, P. M.: On the significance of atmospheric CO_2 growth rate anomalies in 2002–2003, Geophys. Res. Lett., 32, L14816, https://doi.org/10.1029/2005GL023027, 2005.

Keeling, C. D., Adams, J. A., Ekdahl, C. A., and Guenther, P. R.: Atmospheric carbon dioxide variations at the South Pole, Tellus, 28, 552–564, https://doi.org/10.1111/j.2153-3490.1976.tb00702.x, 1976.

Keeling, C. D., Whorf, T. P., Wahlen, M., and van der Plichtt, J.: Interannual extremes in the rate of rise of atmospheric carbon dioxide since 1980, Nature, 375, 666–670, https://doi.org/10.1038/375666a0, 1995.

Keenan, T. F., Prentice, I. C., Canadell, J. G., Williams, C. A., Wang, H., Raupach, M., and Collatz, G. J.: Recent pause in the growth rate of atmospheric CO_2 due to enhanced terrestrial carbon uptake, Nat. Commun., 7, 13428, https://doi.org/10.1038/ncomms13428, 2016.

Le Quéré, C., Raupach, M. R., Canadell, J. G., Marland, G., Bopp, L., Ciais, P., Conway, T. J., Doney, S. C., Feely, R. A., Foster, P., Friedlingstein, P., Gurney, K., Houghton, R. A., House, J. I., Huntingford, C., Levy, P. E., Lomas, M. R., Majkut, J., Metzl, N., Ometto, J. P., Peters, G. P., Prentice, I. C., Randerson, J. T., Running, S. W., Sarmiento, J. L., Schuster, U., Sitch, S., Takahashi, T., Viovy, N., van der Werf, G. R., and Woodward, F. I.: Trends in the sources and sinks of carbon dioxide, Nat. Geosci., 2, 831–836, https://doi.org/10.1038/ngeo689, 2009.

Lintner, B. R., Buermann, W., Koven, C. D., and Fung, I. Y.: Seasonal circulation and Mauna Loa CO_2 variability, J. Geophys. Res., 111, D13104, https://doi.org/10.1029/2005JD006535, 2006.

Liu, F., Beirle, S., Zhang, Q., Dörner, S., He, K., and Wagner, T.: NO_x lifetimes and emissions of cities and power plants in polluted background estimated by satellite observations, Atmos. Chem. Phys., 16, 5283–5298, https://doi.org/10.5194/acp-16-5283-2016, 2016.

Liu, Y., Gruber, N., and Brunner, D.: Spatiotemporal patterns of the fossil-fuel CO_2 signal in central Europe: results from a high-resolution atmospheric transport model, Atmos. Chem. Phys., 17, 14145–14169, https://doi.org/10.5194/acp-17-14145-2017, 2017.

Lucht, W., Prentice, I. C., Myneni, R. B., Sitch, S., Friedlingstein, P., Cramer, W., Bousquet, P., Buermann, W., and Smith, B.: Climatic control of the high-latitude vegetation greening trend and Pinatubo effect, Science, 296, 1687–1689, https://doi.org/10.1126/science.1071828, 2002.

Manning, M. R. and Pohl, K. P.: Atmospheric CO_2 Monitoring in New Zealand 1971-1985, Institute of Nuclear Sciences, DSIR, New Zealand, Report No INS-R-350, 1986.

McClure, C. D., Jaffe, D. A., and Gao, H.: Carbon Dioxide in the Free Troposphere and Boundary Layer at the Mt. Bachelor Observatory, Aerosol Air Qual. Res., 16, 717–728, https://doi.org/10.4209/aaqr.2015.05.0323, 2016.

Möller, D.: Chemistry of the climate system, 2nd fully revised and extended edition, De Gruyter, Berlin, 786 pp., 2017.

Müller, L.: Setup of a combined gas chromatographic system at the stations Schauinsland and Zugspitze for monitoring atmospheric H_2 and other greenhouse gases, University of Heidelberg, 2009.

Nassar, R., Napier-Linton, L., Gurney, K. R., Andres, R. J., Oda, T., Vogel, F. R., and Deng, F.: Improving the temporal and spatial distribution of CO_2 emissions from global fossil fuel emission data sets, J. Geophys. Res., 118, 917–933, https://doi.org/10.1029/2012JD018196, 2013.

Pales, J. C. and Keeling, C. D.: The concentration of atmospheric carbon dioxide in Hawaii, J. Geophys. Res., 70, 6053–6076, https://doi.org/10.1029/JZ070i024p06053, 1965.

Pearman, G. I.: Further studies of the comparability of baseline atmospheric carbon dioxide measurements, Tellus, 29, 171–181, https://doi.org/10.3402/tellusa.v29i2.11343, 1977.

Pearman, G. I. and Garratt, J. R.: Errors in atmospheric CO_2 concentration measurements arising from the use of reference gas mixtures different in composition to the sample air, Tellus, 27, 62–66, https://doi.org/10.3402/tellusa.v27i1.9885, 1975.

Pickers, P. A. and Manning, A. C.: Investigating bias in the application of curve fitting programs to atmospheric time series, Atmos. Meas. Tech., 8, 1469–1489, https://doi.org/10.5194/amt-8-1469-2015, 2015.

R Core Team: R: A Language and Environment for Statistical Computing, Vienna, Austria, available at: https://www.R-project.org/ (last access: 23 January 2019), 2018.

Reiter, R., Sladkovic, R., and Kanter, H.-J.: Concentration of trace gases in the lower troposphere, simultaneously recorded at neighboring mountain stations Part I: Carbon Dioxide, Meteorl. Atmos. Phys., 35, 187–200, https://doi.org/10.1007/BF01041811, 1986.

Schmidt, M., Graul, R., Sartorius, H., and Levin, I.: The Schauinsland CO_2 record: 30 years of continental observations and their implications for the variability of the European CO_2 budget, J. Geophys. Res., 108, ACL 14-1–ACL 14-7, https://doi.org/10.1029/2002JD003085, 2003.

Sirignano, C., Neubert, R. E. M., Rödenbeck, C., and Meijer, H. A. J.: Atmospheric oxygen and carbon dioxide observations from two European coastal stations 2000–2005: continental influence, trend changes and APO climatology, Atmos. Chem. Phys., 10, 1599–1615, https://doi.org/10.5194/acp-10-1599-2010, 2010.

Slemr, F. and Scheel, H. E.: Trends in atmospheric mercury concentrations at the summit of the Wank mountain, Southern Germany, Atmos. Environ., 32, 845–853, https://doi.org/10.1016/S1352-2310(97)00131-3, 1998.

Stephens, B. B., Brailsford, G. W., Gomez, A. J., Riedel, K., Mikaloff Fletcher, S. E., Nichol, S., and Manning, M.: Analysis of a 39-year continuous atmospheric CO_2 record from Baring Head, New Zealand, Biogeosciences, 10, 2683–2697, https://doi.org/10.5194/bg-10-2683-2013, 2013.

Sturm, P., Leuenberger, M., and Schmidt, M.: Atmospheric O_2 CO_2 and $\delta^{13}C$ observations from the remote sites Jungfraujoch, Switzerland, and Puy de Dôme, France, Geophys. Res. Lett., 32, 2467, https://doi.org/10.1029/2005GL023304, 2005.

Thoning, K. W., Tans, P. P., and Komhyr, W. D.: Atmospheric carbon dioxide at Mauna Loa Observatory: 2. Analysis of the NOAA GMCC data, 1974–1985, J. Geophys. Res., 94, 8549, https://doi.org/10.1029/JD094iD06p08549, 1989.

Trickl, T., Cooper, O. R., Eisele, H., James, P., Mücke, R., and Stohl, A.: Intercontinental transport and its influence on the ozone concentrations over central Europe: Three case studies, J. Geophys. Res., 108, STA 15-1–STA 15-23, https://doi.org/10.1029/2002JD002735, 2003.

Trickl, T., Giehl, H., Jäger, H., and Vogelmann, H.: 35 yr of stratospheric aerosol measurements at Garmisch-Partenkirchen: from Fuego to Eyjafjallajökull, and beyond, Atmos. Chem. Phys., 13, 5205–5225, https://doi.org/10.5194/acp-13-5205-2013, 2013.

Tsutsumi, Y., Mori, K., Ikegami, M., Tashiro, T., and Tsuboi, K.: Long-term trends of greenhouse gases in regional and background events observed during 1998–2004 at Yonagunijima located to the east of the Asian continent, Atmos. Environ., 40, 5868–5879, https://doi.org/10.1016/j.atmosenv.2006.04.036, 2006.

Ueyama, M. and Ando, T.: Diurnal, weekly, seasonal, and spatial variabilities in carbon dioxide flux in different urban landscapes in Sakai, Japan, Atmos. Chem. Phys., 16, 14727–14740, https://doi.org/10.5194/acp-16-14727-2016, 2016.

Wang, Y., Munger, J. W., Xu, S., McElroy, M. B., Hao, J., Nielsen, C. P., and Ma, H.: CO_2 and its correlation with CO at a rural site near Beijing: implications for combustion efficiency in China, Atmos. Chem. Phys., 10, 8881–8897, https://doi.org/10.5194/acp-10-8881-2010, 2010.

Watanabe, F., Uchino, O., Joo, Y., Aono, M., Higashijima, K., Hirano, Y., Tsuboi, K., and Suda, K.: Interannual Variation of Growth Rate of Atmospheric Carbon Dioxide Concentration Observed at the JMA's Three Monitoring Stations: Large Increase in Concentration of Atmospheric Carbon Dioxide in 1998, J. Meteorol. Soc. Jpn., 78, 673–682, 2000. The link to the data has been updated. Please change the link as below,

World Data Centre for Greenhouse Gases (WDCGG): Global monthly mean mole fractions, available at: https://gaw.kishou.go.jp/publications/global_mean_mole_fractions, last access: 23 January 2019a.

World Data Centre for Greenhouse Gases (WDCGG): Greenhouse gases and related gases (CO_2, CO, NO), available at: https://gaw.kishou.go.jp/, last access: 23 January 2019b.

Winkler, P., Lugauer, M., and Reitebuch, O.: Alpine Pumping, Promet, 32, 34–42, 2006.

WMO Greenhouse Gas Bulletin: The State of Greenhouse Gases in the Atmosphere Based on Global Observations through 2017, World Meteorological Organization, Geneva, No. 14, 2018.

Yuan, Y., Ries, L., Petermeier, H., Steinbacher, M., Gómez-Peláez, A. J., Leuenberger, M. C., Schumacher, M., Trickl, T., Couret, C., Meinhardt, F., and Menzel, A.: Adaptive selection of diurnal minimum variation: a statistical strategy to obtain representative atmospheric CO_2 data and its application to European elevated mountain stations, Atmos. Meas. Tech., 11, 1501–1514, https://doi.org/10.5194/amt-11-1501-2018, 2018.

Zhang, F., Zhou, L., Conway, T. J., Tans, P. P., and Wang, Y.: Short-term variations of atmospheric CO_2 and dominant causes in summer and winter: Analysis of 14-year continuous observational data at Waliguan, China, Atmos. Environ., 77, 140–148, https://doi.org/10.1016/j.atmosenv.2013.04.067, 2013.